NANO LETTERS

2003
Vol. 3, No. 12
1683−1686

Nanosignal Processing: Stochastic Resonance in Carbon Nanotubes That Detect Subthreshold Signals

Ian Y. Lee, Xiaolei Liu, Bart Kosko,* and Chongwu Zhou

Electrical Engineering Department, University of Southern California, Los Angeles, California 90089-2564

Received September 25, 2003; Revised Manuscript Received October 11, 2003

ABSTRACT

Experiments confirm that small amounts of noise help a nanotube transistor detect noisy subthreshold electrical signals. Gaussian, uniform, and impulsive (Cauchy) noise produced this feedforward stochastic-resonance effect by increasing both the nanotube system's mutual information and its input–output correlation. The noise corrupted a synchronous Bernoulli or random digital sequence that fed into the thresholdlike nanotube transistor and produced a Bernoulli sequence. Both Shannon's mutual information and correlation measured the performance gain by comparing the input and output sequences. This nanotube SR effect was robust: it persisted even when infinite-variance Cauchy noise corrupted the signal stream. Such noise-enhanced signal processing at the nanolevel promises applications to signal detection in wideband communication systems and biological and artificial neural networks.

Noise can help carbon nanotube transistors detect subthreshold electrical signals by increasing the transistor's input−output mutual information or correlation. Several researchers have demonstrated the stochastic resonance (SR) effect for various types of threshold units or neurons.[1−6] Experiments with p-type nanotube transistors confirmed the specific SR prediction based on the theoretical finding that simple memoryless threshold neurons exhibit SR for almost all finite-variance and infinite-variance noise types.[7] The experiments used three types of additive noise (Gaussian, uniform, and infinite-variance[1] Cauchy noise) and different combinations of subthreshold ON/OFF electrical signals. Figure 1 shows the nonmonotonic signature of SR for white Gaussian noise and the thresholdlike nonlinearity of the nanotube transistors.[8−13] The modes of the mutual-information and correlation curves occurred for nonzero noise strength with a standard deviation of at least 0.01.

The nanotube experiments produced the SR effect for both the Shannon mutual information and the input−output correlation[14] of noisy Bernoulli sequences. The mutual information $I(S, Y)$ subtracts the noisy channel's (the transistor's) output conditional entropy $H(Y|S)$ from its unconditional entropy $H(Y)$: $I(S, Y) = H(Y) - H(Y|S)$. The input signal S was a random binary voltage that produced a random output Y in the form of a transistor current. The correlation measure found the normalized zero-lag cross-correlation

$$r_{SY}(l) = \sum_{k=1}^{N} s(k)\, y(k - l)$$

of the two sequences with subtracted means. The measures did not assume that the nanotube detector had a special structure and did not impose a threshold scheme on the experiment.

Figure 1b shows the thresholdlike nonlinearity of the nanotube transistor in response to the noisy input signal. The transconductance G related the output drain-to-source current I to the input gate voltage V and the threshold voltage V_T in a memoryless signal function: $I = G\,(V - V_T)$ if $V \le V_T$ and zero otherwise. We note that the threshold neuron model lacks the internal state dynamics of the FitzHugh−Nagumo (FHN) model.[15] The transconductance G was negative because the pristine (undoped) nanotube transistors exhibited current−voltage characteristics that were consistent with p-type transistors. Linear regression extrapolated the nonlinearity and estimated the threshold voltage.

Each of the nanotube experiments (Supporting Information) applied 32 independent trials of 1000-symbol input sequences for 24 noise levels per type and over a range of gate voltages. The 24 sampled noise levels ranged from 0.001 to 1 standard deviation (dispersion for infinite-variance Cauchy) linearly on a logarithmic scale. The noisy input was

* Corresponding author. E-mail: kosko@sipi.usc.edu.

10.1021/nl0348239 CCC: $25.00
Published on Web 11/11/2003

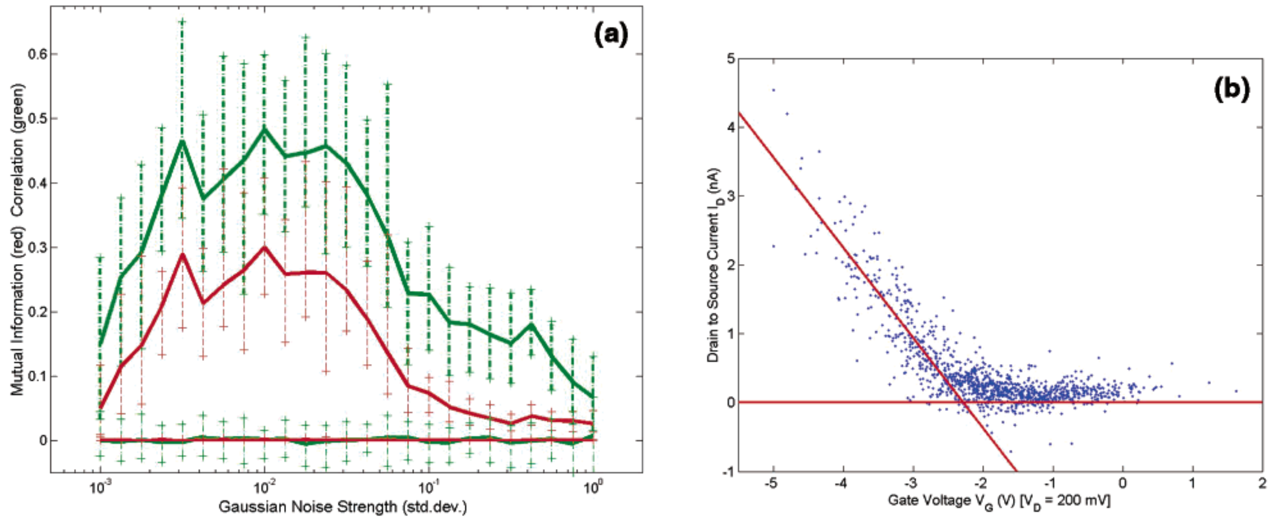

Figure 1. (a) Stochastic resonance with additive white Gaussian noise. The CNT-FET detector's mutual information (top red curve) and zero-lag correlation (top green curve) increase for small amounts of noise and then decrease for larger amounts. The control experiments gave the flat non-SR mutual information (bottom red curve) and correlation (bottom green curve) when no nanotube bridged the source and drain electrodes. The SR mode or optimal noise level had the same standard deviation value of 0.01 for both performance measures. Each vertical dashed bar occurs at 1 of the 24 sampled noise values and shows the maximum and the minimum range of 32 averaged experimental trials. The solid polygonal line connects the means of those 24 sets of experiments. The random input sequence S was a Bernoulli sequence of ON/OFF values with additive white Gaussian noise. The random sequence Y was the output of the nanotube threshold detector. Shown is one of four such successful combinations of input binary values with the parameter choices ON = −1.6 V and OFF = −1.4 V. Each trial applied 1000 subthreshold symbols to the detector. The input signal was the analog voltage representation of the symbol sequence S at approximately 10-ms intervals. The output signal was the nanotube current. The data acquisition measured and averaged 10 samples at 100 ksamples/s near the end of each symbol interval to estimate the output sequence (Supporting Information). A χ^2 test and a Kolmogorov−Smirnov test both rejected the similarity between a monotonically decreasing β probability density function and the two SR curves ($p < 0.001$). (b) Thresholdlike (nonlinear) gate effect of the p-type CNT-FET detector. Each point shows the detector's response to one random input symbol. The experimental data showed that the CNT-FET detector behaved as a threshold in response to the noisy input signal stream. The gate effect showed little hysteresis. This differed from the hysteretic curve that a semiconductor parameter analyzer captured from the detector (Supporting Information) and differed from the typical hysteretic loops in ref 18. Linear regression gave an approximate threshold gate voltage of $V_T = -2.3$ V ($\beta_0 = -2.99$ nA, $\beta_1 = -1.31$ nA/V, p value < 0.0001) for the transistor current equation $I = G(V - V_T)$ if $V \leq V_T$ and zero otherwise.

a synchronized Bernoulli sequence of independent random (subthreshold) ON/OFF values and additive white noise of three types. So there was no timing noise in the pulse train as in the FHN neuron model.[16] The discrete-time noise was white because the noise samples were uncorrelated in time. So the discrete-time Fourier transform was 2π-periodic and produced a flat noise power spectrum over the interval $[0, 2\pi]$.[17,18] Synchronization allows the nanotube systems to implement a variety of algorithms from signal processing and communications.

The ON/OFF values in Figure 1a were ON = −1.6 V and OFF = −1.4 V. The input updated the symbols about once every 10 ms. A 200-mV drain-source voltage biased the nanotube at room temperature in vacuum. The experiment measured and averaged 10 samples of the detector output at 100 ksymbols/s near the end of each symbol interval to estimate the output sequence.

A histogram of the output sequence gave the discrete probability density function $P(Y = Y_i) = p_i$ that computed the unconditional Shannon entropy:

$$H(Y) = -\sum_{i=1}^{N} p_i \ln p_i \tag{1}$$

for mutual information without converting the detector output into a binary sequence with a threshold scheme. Sorting the output sequence based on the input symbol and then applying the histogram gave the conditional output discrete probability density function $P_{Y|S}(Y = Y_i|S = S_j) = p_{ji}/p_j$ conditioned on the input symbols that computed the conditional entropy:

$$H(Y|S) = -\sum_{i=1}^{N}\sum_{j=1}^{N} p_{ji} \ln\left(\frac{p_{ji}}{p_j}\right) \tag{2}$$

The mutual information measure was the difference between the unconditional and conditional entropies:

$$I(S, Y) = H(Y) - H(Y|S) \tag{3}$$

Cross correlation compared the input and the output symbol sequences and gave a scalar representation with its zero-lag value:

$$r_{SY}(0) = \sum_{k=1}^{N} s(k)\, y(k) \tag{4}$$

Converting the input Bernoulli sequence to bipolar form (mapping ON to +1 and OFF to −1) made it approximately

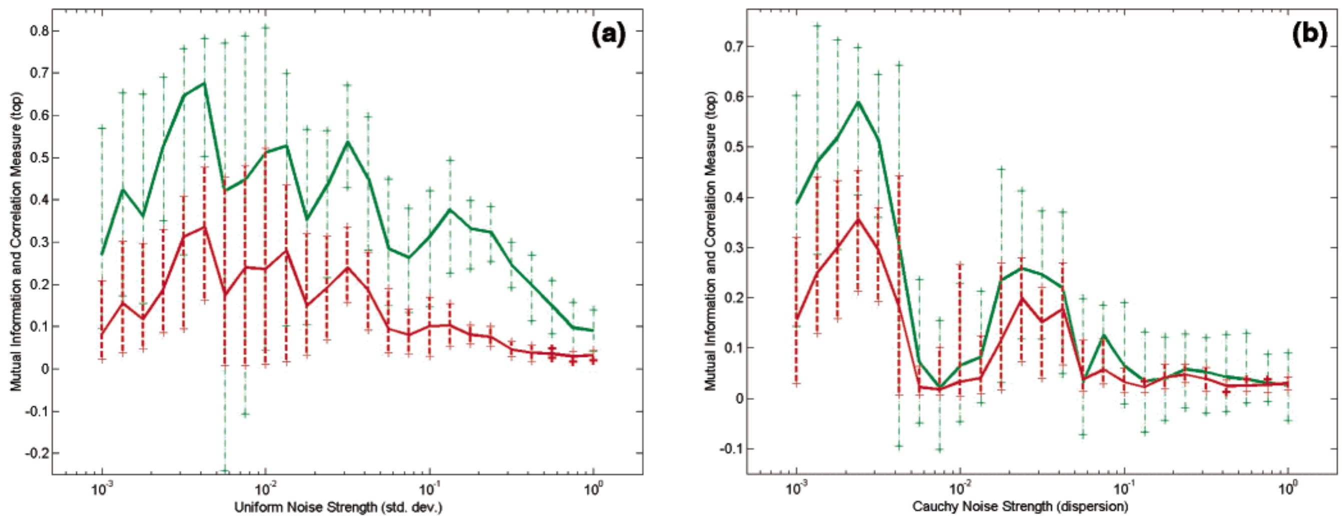

Figure 2. (a) Stochastic resonance with additive white uniform noise. All four combinations of input voltage values produced a clear SR response in both mutual information (bottom red curve) and input−output correlation (top green curve) just as with additive white Gaussian noise. Shown is the SR effect for the subthreshold signal ON = −1.8 V and OFF = −1.6 V. The SR mode is at 0.04 standard deviation. (b). Robust stochastic resonance with additive white Cauchy noise. This highly impulsive noise has infinite variance and infinite higher-order moments. The Cauchy-noise experiment produced a measurable SR effect for two of the four combinations of input voltages. Shown is an approximate SR effect for the subthreshold signal ON = −2 V and OFF = −1.8 V. The SR mode lies at about the 0.003 dispersion value. Several SR researchers have found multiple modes in the plot of system performance against noise strength.[51−53] The limited dynamic range [−5V, 5V] of the data acquisition equipment (Supporting Information) may have produced the second peak in the graph as a truncation artifact because it clipped large spikes when it realized the infinite-variance Cauchy noise. The clipping affected more than 0.1% of the noise only for dispersions greater than 0.01.

zero mean (equal numbers of +1's and −1's give exactly zero mean) and noise-free. Subtracting the sample mean from the output sequence improved the match between similar input and output sequences. A normalization scheme gave the normalized correlation measure:[14]

$$C(S, Y) = \frac{\sum_{k=1}^{N} s(k)\, y(k)}{\sqrt{\sum_{k=1}^{N} s(k)\, s(k)}\sqrt{\sum_{k=1}^{N} y(k)\, y(k)}} \qquad (5)$$

It divided the zero-lag cross correlation $r_{SY}(0)$ by the square root of the energy of the input and the output sequences where the energy of a sequence is the same as the zero-lag value of its autocorrelation:

$$|x| = \sum_{k=1}^{N} x^2(k) = \sum_{k=1}^{N} x(k)\, x(k-l)|_{l=0} = r_{XX}(0) \qquad (6)$$

Nanotube field-effect transistor technology produced detectors that could exhibit hysteresis[19−21] or react to adsorbed molecules.[22−24] The experiment applied subthreshold symbols that were at least two standard deviations away from the far leg of the hysteretic loop. The effective $I - V_G$ curve in Figure 1b, as collected from the detector response to the input symbols, showed that the experiment produced evidence of the SR effect despite the potential hysteretic effect.

The experiment found the SR effect for mutual information and correlation for Gaussian and uniform noise and for four combinations of binary symbols: (−2.0, −1.8), (−1.8, −1.6), (−1.6, −1.4), and (−1.4, −1.2) V. Figure 1a shows the SR effect for additive white Gaussian noise and the subthreshold signal pair ON = −1.6 V and OFF = −1.4 V. The SR mode of the mutual-information curve is 6 times the value at minimal noise. The SR mode of the correlation curve is 3 times the value at minimal noise. Figure 2a shows the SR effect for additive white uniform noise and the signal pair ON = −1.8 V and OFF = −1.6 V.

We also passed impulsive or infinite-variance white noise through the nanotube detector to test whether it was robust to occasional large noise spikes. We chose the highly impulsive Cauchy noise[1] for this task. This infinite-variance noise probability density function had the form

$$p(n) = \frac{\gamma}{\pi(n^2 + \gamma^2)}$$

for zero location and finite dispersion γ. Figure 2b shows that a diminished SR effect still persists for Cauchy noise with the subthreshold signal pair ON = −2.0 V and OFF = −1.8 V. Not all Cauchy experiments produced a measurable SR effect.

These SR results suggest that nanotubes can exploit noise in other signal-processing tasks if advances in nanotube device technology can overcome the problems of hysteresis and parasitic capacitance that affect logic circuits[25] and high-frequency signals.[26] The nanotube signal detectors might apply to broadband[27,28] or optical communication systems[29] that use submicroamp currents and attenuated signals in noise because our nanotube detectors used nanoamp current and could distinguish between subthreshold binary symbols. The detectors might apply to parallel signal processing[30] at the nanolevel because they could have a small minimum feature size[31] in vast parallel arrays of nanotubes. The parallel detectors could apply to spread spectrum communications: each nanotube can act as an antenna[32] that matches a separate frequency channel[33] in frequency hopping and perhaps in other types of spread spectrum communications.[34] A nanotube's length can code for a given frequency[35] while chemical adsorption can tune a nanotube's threshold.[23,24] The detectors might apply to chemical detection and parallel field programming by tuning the threshold chemically. The nanotube detectors can also operate in a biological environment such as saline solution.[36] The nanotube detectors could interface with biological systems because an electrolyte can act as their gate.[36,37] The nanotube detectors might also help implement pulse-train neural networks and exploit noise in biological[38−49] or robotic systems because the detectors are threshold devices similar to spiking neurons.[50]

Acknowledgment. The National Science Foundation (grant no. ECS-0070284) supported this research. We thank Chao Li, Sanya Mitaim, and Ashok Patel for helpful discussions.

Supporting Information Available: Methods and Materials. This material is available free of charge via the Internet at http://pubs.acs.org.

References

(1) Kosko, B.; Mitaim, S. *Neural Networks* **2003**, *16*, 755.
(2) Kosko, B.; Mitaim, S. *IJCNN'02 IEEE Proc. Int. Joint Conf. Neural Networks*; **2002**, *2*, 1980.
(3) Moss, F.; Pierson, D.; O'Gorman, D. *Int. J. Bifurc. Chaos* **1994**, *6*, 1383−1397.
(4) Gingl, Z.; Kiss L.; Moss, F. *Europhys. Lett*. **1995**, *29*, 191.
(5) Inchiosa, M. E.; Robinson, J. W. C.; Bulsara, A. R. *Phys. Rev. Lett*. **2000**, *85*, 3369−3372.
(6) Gammaitoni, L.; Bulsara, A. R. *Phys. Rev. Lett.* **2002**, *88*, 230601
(7) Kosko, B.; Mitaim, S. *Phys. Rev. E* **2001**, *64*, 051110.
(8) Tans, S. J.; Verschueren, R. M.; Dekker, C. *Nature* **1998**, *393*, 49.
(9) Zhou, C.; Kong, J.; Dai, H. *Appl. Phys. Lett.* **2000**, *76*, 1597.
(10) Martel, R.; Schmidt, T.; Shea, H. R.; Hertel, T.; Avouris Ph. *Appl. Phys. Lett*. **1998**, *73*, 2447.
(11) Cheung, C. L.; Kurtz, A.; Park, H.; Lieber, C. M. *J. Phys. Chem. B* **2002**, *106*, 2429.
(12) Liu, J.; Rinzler, A. G.; Dai, H.; Hafner, J. H.; Bradley, R. K.; Boul, P. J.; Lu, A.; Iverson, T.; Shelimov, K.; Huffman, C. B.; Rodriguez-Macias, F.; Shon, Y. S.; Lee, T. R.; Colbert, D. T.; Smalley, R. E. *Science* **1998**, *280*, 1253−1256.
(13) Saito, R.; Fujita, M.; Dresselhaus, G.; Dresselhaus, M. S. *Appl. Phys. Lett.* **1992**, *60*, 2204.
(14) Collins, J. J.; Chow, C. C.; Capela, A. C.; Imhoff, T. T. *Phys. Rev. E* **1996**, *54*, 5575.
(15) Pei, X.; Bachmann, K.; Moss, F. *Phys. Lett. A*, **1995**, *206*, 61−65.
(16) Pei, X.; Wilkens, L.; Moss, F. *Phys. Rev. Lett.* **1996**, *77*, 4679−4682.
(17) Oppenheim, A. V.; Schafer, R. W.; Buck, J. R. *Discrete-Time Signal Processing*, 2nd ed.; Prentice-Hall: Upper Saddle River, NJ, 1999.
(18) Ingle, V. K.; Manolakis, D. G.; Kogon, S. *Statistical and Adaptive Signal Processing: Spectral Estimation, Signal Modeling, Adaptive Filtering and Array Processing*; McGraw-Hill: New York, 1999
(19) Kim, W.; Javey, A.; Vermesh, O.;Wang, Q.; Li, Y.; Dai, H. *Nano Lett.* **2003**, *3*, 193.
(20) Fuhrer, M. S.; Kim, B. M.; Durkop, T.; Bringlinger, T. *Nano Lett*. **2002**, *2*, 757.
(21) Radosavljevic, M.; Freitag, M.; Thadani, K. V.; Johnson, A. T. *Nano Lett*. **2002**, *2*, 761.
(22) Ong, K. G.; Zeng, K.; Grimes, C. A. *IEEE Sensors J.* **2002**, *2*, 82.
(23) Collins, P. G.; Bradley, K.; Ishigami, M.; Zettl, A. *Science* **2000**, *287*, 1801.
(24) Kong, J.; Franklin, N. R.; Zhou, C.; Chapline, M. G.; Peng, S.; Cho, K.; Dai, H. *Science* **2000**, *287*, 622−625.
(25) Bachtold, A.; Hadley, P.; Nakanishi, T.; Dekker, C. *Science* **2001**, *294*, 1317.
(26) Harris, D.; Horowitz, M. A. *IEEE J. Solid-State Circuits* **1997**, *32*, 1702−1711.
(27) Bulsara, A. R.; Zador, A. *Phys. Rev. E* **1996**, *54*, R2185.
(28) Barbay, S.; Giacomelli, G.; Marin, F. *Phys. Rev. E* **2000**, *63*, 051110−051118.
(29) Chen, Y.-C.; Raravikar, N. R.; Schadler, L. S.; Ajayan, P. M.; Zhao, Y.-P.; Lu, T.-M.; Wang, G.-C.; Zhang, X.-C. *Appl. Phys. Lett*. **2002**, *81*, 975−977.
(30) Stocks, N. G. *Phys. Rev. E* **2001**, *63*, 041114−041122.
(31) Rochefort, A.; Ventra, M. D.; Avouris, Ph. *Appl. Phys. Lett.* **2001**, *78*, 2521.
(32) Liang, W.; Bockrath, M.; Bozovic, D.; Hafner, J. H.; Tinkham, M.; Park, H. *Nature* **2001**, *411*, 665−669.
(33) Blake, L. V. *Antennas*, 2nd ed.; Artech House Inc.: Dedham, MA, 1984.
(34) Irmer R.; Fettweis, G. In *The 5th International Symposium on Wireless Personal Multimedia Communications*; IEEE: Washington, D.C., 2002; Vol. 2, Iss. 27−30, pp 412−416.
(35) Huang, S.; Cai, X.; Liu, J. *J. Am. Chem. Soc.* **2003**, *125*, 5636−5637.
(36) McEuen, P. L.; Fuhrer, M. S.; Park, H. *IEEE Trans. Nanotech.* **2002**, *1*, 78.
(37) Kruger, M.; Buitelaar, M. R.; Nussbaumer, T.; Schonenberger, C.; Forro, L. *Appl. Phys. Lett.* **2001**, *78*, 1291.
(38) Russel, D. F.; Wilkens, Lon. A.; Moss, F. *Nature* **1999**, *402*, 291.
(39) Jaramillo, F.; Wiesenfeld, K. *Nat. Neurosci.* **1998**, *1*, 384.
(40) Bulsara, A. R.; Boss, R. D.; Jacobs, E. W. *Biol. Cybern.* **1989**, *61*, 211−222.
(41) Pantazelou, E.; Dames, C.; Moss, F.; Douglass, J.; Wilkens, L. *Int. J. Bifurc. Chaos* **1995**, *5*, 101−108.
(42) Pei, X.; Wilkens, L.; Moss, F. *J. Neurophysiol.* **1996**, *76*, 3002−3011.
(43) Douglass, J. K.; Wilkens, L.; Pantazelou, E.; Moss, F. *Nature* **1993**, *365*, 337−340.
(44) Levin, J. E.; Miller, J. P. *Nature* **1996**, *380*, 165−168.
(45) Miller, J. P.; Jacobs, G. A.; Theunissen, F. E. *J. Neurophysiol.* **1991**, *66*, 1680−1689.
(46) Miller, J. P.; Jacobs, G. A.; Theunissen, F. E. *J. Neurophysiol.* **1991**, *66*, 1690−1703.
(47) Braun, H. A.; Wissing, H.; Schäfer, K.; Hirsch, M. C. *Nature* **1994**, *367*, 270−273.
(48) Gluckman, B. J.; Netoff, T. I.; Neel, E. J.; Ditto, W. L.; Spano, M. L.; Schiff, S. J. *Phys. Rev. Lett.* **1996**, *77*, 4098−4101.
(49) Collins, J. J.; Imhoff, T. T.; Grigg, P. *J. Neurophysiol.* **1996**, *76*, 642−645.
(50) Rieke, F.; Warland, D.; Steveninck, RdRv. *Spikes: Exploring the Neural Code*; MIT Press: Cambridge, MA, 1999.
(51) Vilar, J. M. G.; Rubí, J. M. *Phys. Rev. Lett*. **1997**, *78*, 2882−2885.
(52) Lindner, J. F.; Breen, B. J.; Wills, M. E.; Bulsara, A. R.; Ditto, W. L. *Phys. Rev. E* **2001**, *63*, 051107.
(53) Matyjaskiewicz, S.; Krawiecki, A.; Holyst, J. A.; Kacperski, K.; Ebeling, W. *Phys. Rev. E* **2001**, *63*, 026215.

NL0348239